MOLECULAR AND CELLULAR BIOLOGY, Sept. 1997, p. 4967–4978 Vol. 17, No. 9
0270-7306/97/$04.00+0

Identification of Putative c-Myc-Responsive Genes: Characterization of *rcl*, a Novel Growth-Related Gene†

BRIAN C. LEWIS,[1,2] HYUNSUK SHIM,[1] QING LI,[3] CHYI SUN WU,[1] LINDA A. LEE,[1] AMIT MAITY,[1] AND CHI V. DANG[1,2,3,4,5]*

Department of Medicine,[1] Department of Molecular Biology and Genetics,[4] Johns Hopkins Oncology Center,[5] Program in Human Genetics and Molecular Biology,[2] and Program in Cellular and Molecular Medicine,[3] The Johns Hopkins University School of Medicine, Baltimore, Maryland 21205

Received 3 January 1997/Returned for modification 19 February 1997/Accepted 5 June 1997

The c-Myc protein is a helix-loop-helix leucine zipper oncogenic transcription factor that participates in the regulation of cell proliferation, differentiation, and apoptosis. The biochemical function of c-Myc has been well described, yet the identities of downstream effectors are just beginning to emerge. We describe the identification of a set of c-Myc-responsive genes in the Rat1a fibroblast through the application of cDNA representational difference analysis (RDA) to cDNAs isolated from nonadherent Rat1a and Rat1a-myc cells. In this system, c-Myc overexpression is sufficient to induce the transformed phenotype of anchorage-independent growth. We identified 20 differentially expressed cDNAs, several of which represent novel cDNA sequences. We further characterized one of the novel cDNAs identified in this screen, termed *rcl*. *rcl* expression is (i) directly stimulated by c-Myc; (ii) stimulated in the in vivo growth system of regenerating rat liver, as is c-*myc*; and (iii) elevated in human lymphoid cells that overexpress c-*myc*. By using an anti-Rcl antibody, immunoblot analysis, and immunofluorescence microscopy, the Rcl protein was found to be a 23-kDa nuclear protein. Ectopic expression of the protein encoded by the *rcl* cDNA induces anchorage-independent growth in Rat1a fibroblasts, albeit to a diminished extent compared to ectopic c-Myc expression. These data suggest a role for *rcl* during cellular proliferation and c-Myc-mediated transformation.

The c-*myc* proto-oncogene encodes a helix-loop-helix leucine zipper transcription factor that participates in the regulation of cell proliferation, differentiation, and apoptosis (6, 9, 10, 21, 31, 45, 57). Deregulation of c-*myc* expression has been found in Burkitt's lymphoma and other human neoplasms (11, 32, 41). c-Myc forms a heterodimer with its partner protein Max (6). Together they bind to the specific DNA sequences CAC(A/G)TG or E-box and activate transcription (6, 9, 11, 45). The domains necessary for DNA binding and transcriptional activation have been well defined by previous studies performed in several laboratories. c-Myc has also been shown to interact with TFII-I and impede transcription from the initiator element (33, 35, 44, 47, 48, 55).

Although the biochemical function of c-Myc has been well described, the identities of downstream effectors are just beginning to emerge. Among the candidate c-Myc target genes are those encoding ornithine decarboxylase (ODC), prothymosin α, CDC 25A, eIF4E, ECA39, and MrDb (2, 3, 15, 18, 20, 30, 43, 59). Previous approaches to the identification of c-Myc targets have been based on two main strategies. The first approach is differential cloning or subtractive hybridization, and the second involves identifying targets based on the biological effects of c-Myc expression. Prothymosin α and ECA39 have been identified as potential c-Myc targets by the first strategy (5, 15). ODC, dihydrofolate reductase, and carbamoyl-phosphate synthetase have been proposed as c-Myc targets in studies involving the second approach (2, 3, 39, 40, 43, 59). Grandori et al. have recently described the identification of c-Myc target genes by coimmunoprecipitation of chromatin-bound Myc/Max complexes (20). While some of the previous studies have yielded potentially physiological targets of c-Myc and valuable insights into c-Myc function, some of these putative targets, such as ECA39 and prothymosin α, show a cell-type-specific response to c-Myc and have not been placed in the biological context of c-Myc-mediated transformation (4, 19, 58). We therefore sought to identify genes that act downstream of c-Myc in a biologically relevant system.

In this report, we describe the identification of a set of putative c-Myc-responsive genes in Rat1a fibroblasts, which can be transformed to display anchorage-independent growth in soft agar by overexpression of c-Myc alone (Rat1a-myc cells) (56). These genes were identified by the application of cDNA representational difference analysis (RDA) to cDNAs isolated from nonadherent Rat1a and Rat1a-myc cells, which were grown on an agarose layer to mimic anchorage-independent growth conditions (28, 37). We hypothesized that genes differentially expressed between Rat1a and Rat1a-myc cells under nonadherent conditions contribute to the anchorage-independent growth phenotype of Rat1a-myc cells. The collection of genes identified includes previously described targets of c-Myc including the ODC gene, as well as several novel genes and known genes not previously linked to c-Myc.

We describe the characterization of one of the novel cDNAs identified in this screen, termed *rcl*. *rcl* expression is (i) stimulated by c-Myc; (ii) stimulated in the in vivo growth system of regenerating rat liver, as is c-*myc*; and (iii) elevated in human lymphoid cells that overexpress c-*myc*. *rcl* encodes a 23-kDa nuclear protein of unknown function; however, its ectopic expression induces anchorage-independent growth in Rat1a fibroblasts, albeit to a diminished extent compared to Rat1a-Myc. These data suggest a role for *rcl* during cellular proliferation and c-Myc-mediated transformation phenotypes. Our studies therefore indicate that RDA is a reliable method for cloning differentially expressed genes and that the genes identified in

* Corresponding author. Mailing address: Ross Research Building, Room 1025, Johns Hopkins School of Medicine, 720 Rutland Ave., Baltimore, MD 21205. Phone: (410) 955-2773. Fax: (410) 955-0185. E-mail: cvdang@welchlink.welch.jhu.edu.

† Dedicated to the memory of Calvin Lewis.

our study may provide further clues to the mechanisms by which c-Myc stimulates cellular transformation.

MATERIALS AND METHODS

Cell lines. Rat1a and Rat1a-myc cell lines have been described previously (26, 56). Unless otherwise indicated, these cell lines were cultured in Dulbecco's modified Eagle's medium (DMEM) with 10% fetal bovine serum, penicillin (100 U/ml), and streptomycin (100 μg/ml). Stable cell lines were generated by Lipofectin (GIBCO-BRL, Grand Island, N.Y.)-mediated transfection for 6 h in OptiMEM (GIBCO-BRL) as specified by the manufacturer. The Rat1a-*rcl* and Rat1a-pSG5 cell lines were generated by cotransfection of either pSG5-*rcl* or pSG5 and the puromycin resistance plasmid pBabe-puro (13) at a 20:1 plasmid weight ratio. Pools of resistant colonies were generated by selection in 0.75 μg of puromycin per ml in DMEM. Human lymphoblastoid and Burkitt's lymphoma cells were cultured as previously described (38).

Cell cycle analysis. Rat1a and Rat1a-myc cells were grown for 48 h on plates coated with 0.7% agarose as described previously (1). Following incubation for 30 min with the nucleotide analog bromodeoxyuridine (BrdU) (10 mM), the cells were washed in phosphate-buffered saline and fixed in 70% ethanol at −20°C, digested with pepsin (0.4 mg/ml in 0.1 N HCl) for 30 min at room temperature (50), and stained with a fluorescein isothiocyanate-labeled anti-BrdU antibody (Becton Dickinson Immunocytometry Systems, San Jose, Calif.); then the total DNA was stained with propidium iodide. Propidium iodide and fluorescein isothiocyanate fluorescence and forward light scattering were detected with a Coulter EPICS 752 flow cytometer equipped with MDADS 11 software, version 1.0. Cell cycle distribution profiles were determined with the curve-fitting program Elite version 3.0 (Coulter, Hialeah, Fla.).

RDA. Cells (2×10^6) from either Rat1a or Rat1a-myc cell lines were plated on 150-mm plates coated with a layer of 0.7% agarose in DMEM and were grown for 48 h. mRNA was isolated by guanidium thiocyanate lysis followed by cesium chloride centrifugation and then by poly(A)$^+$ selection on an oligo(dT) column as described previously (49). cDNA was then synthesized with the RiboClone cDNA synthesis kit (Promega, Madison, Wis.). The cDNAs were then digested with either *Dpn*II or *Sau*3A and subjected to RDA as previously described (7, 28, 37), with the following modifications: (i) PCR conditions were 95°C for 5 min, 95°C for 1 min, 65°C for 1 min, and 72°C for 3 min; and (ii) mung bean nuclease was extracted with phenol-chloroform instead of being heat inactivated, as recommended by the manufacturer.

RDA-selected amplicons were then either (i) digested with *Dpn*II, run on a 1% agarose gel, excised as individual bands, and subcloned into *Bam*HI-digested pBluescript KS or (ii) subcloned directly into PCR 2.1 via TA cloning (Invitrogen, San Diego, Calif.). Subcloned amplicons were then ^{32}P labeled and hybridized to slot blots of Rat1a and Rat1a-myc amplicons. Those that were differentially represented were called differential amplicons and then tested by Northern blot analysis or an RNase protection assay.

RNase protection assays. For rat organs, total RNA was isolated by guanidium thiocyanate lysis followed by cesium chloride centrifugation as previously described (49). For Rat1a and Rat1a-myc cells, total RNA was isolated with the RNAid Plus kit (BIO 101, Vista, Calif.). For regenerating rat liver, total RNA samples were obtained as gifts from Anna Mae Diehl (Johns Hopkins University, Baltimore, Md.). A 10-μg amount of total RNA was used in the RNase protection assay with the RPA II kit (Ambion, Austin, Tex.) as specified by the manufacturer. Probes were transcribed from M2B4 (*rcl*), M2A9 (vimentin), and RMyc (a 300-bp fragment from exon 2 amplified with primers RMyc1 [5′ CCATACTTCATGTGCGACGA 3′] and RMyc2 [5′ CCTGCAGAATGATGT TCTTC 3′] from a Stratagene rat liver cDNA library).

Northern blot analysis. Poly(A)$^+$ RNA from Rat1a and Rat1a-myc cells was generated as described for RDA above. A 2-μg portion of poly(A)$^+$ RNA was loaded per lane on a 1.2% agarose–formaldehyde gel. After transfer to nitrocellulose, the blot was probed with ^{32}P-labeled 260-bp M2B4 fragment and then washed twice with 2× SSC (1× SSC is 0.15 M NaCl plus 0.015 M sodium citrate)–0.1% sodium dodecyl sulfate (SDS) for 10 min at room temperature and twice with 0.2× SSC–0.1% SDS for 30 min at 50°C.

The Rat1a Myc-estrogen receptor (ER) cells (a gift of J. M. Bishop, University of California, San Francisco, Calif.) were grown to confluence in DMEM–10% fetal bovine serum and then grown for 2 days in phenol red-free medium with 10% charcoal-treated fetal bovine serum (Hyclone, Logan, Utah). To induce c-Myc activity, Myc-ER cells grown to confluence were exposed to 0.25 μM 4-hydroxytamoxifen (Research Biochemical International, Natrick, Mass.) for the indicated times as previously described (20). To block protein synthesis, these cells were exposed to 10 μM cycloheximide (Sigma Chemical Co., St. Louis, Mo.) 30 min before the addition of hydroxytamoxifen. Total RNA was isolated by guanidium lysis and cesium chloride centrifugation. A 15-μg portion of RNA was loaded per lane on an agarose-formaldehyde gel. After transfer, the blot was hybridized with an *rcl* cDNA probe and normalized with a murine ribosomal protein *rpL32* cDNA (a gift of R. Muschel, University of Pennsylvania, Philadelphia, Pa.) or vimentin cDNA probe. rpL32 mRNA encodes a ribosomal protein and is an mRNA whose level does not vary during the cell cycle. A PhosphorImager (Molecular Dynamics, Sunnyvale, Calif.) was used for quantitation of radiolabeled signals.

Plasmids. The vector pHA-2Hyb is an expression vector which places sequences encoding a hemagglutinin (HA) tag 5′ (at the amino terminus) of the protein-coding sequence. pHA-2Hyb was constructed with the pGalO vector backbone, into which the pBluescript polylinker was inserted. The polylinker was modified by subcloning an oligonucleotide encoding the HA tag at the 5′ end of the polylinker. pHA-*rcl* was created by PCR amplification of *rcl* cDNA clone C5 with the primers pHACBL 5′ and pHACBL 3′, which introduced *Sal*I and *Not*I sites at the 5′ and 3′ ends of the cDNA, respectively. This PCR product was then cloned into the *Sal*I and *Not*I sites of pHA-2Hyb, and clones were sequenced.

pSG5-*rcl* was created by cloning the 5′ *Eco*RI-*Sty*I fragment of C5 and the 3′ *Sty*I-*Bam*HI fragment of C6 into the *Eco*RI and *Bgl*II sites of pSG5 (Stratagene, La Jolla, Calif.).

cDNA library screen. An adult rat liver cDNA library (Stratagene) was screened with the ^{32}P-labeled M2B4 fragment as a probe. A total of 10^6 PFU at a density of 50,000 PFU/plate was screened in the primary screen. Three positive clones were then purified through secondary, tertiary, and quaternary screens. cDNAs in pBluescript SK were then obtained by in vivo excision with helper phage as specified by the manufacturer. The identity of these clones were then tested by PCR with primers M2B4L (5′-AAGGTGCTCACTGAGCACGT 3′) and M2B4R (5′ AAGCACTCGGCCAGACTGTG 3′) and also sequenced with these primers.

Generation of antibodies. *rcl* cDNA was PCR amplified with primers pHACBL 5′ and pHACBL 3′ and then cloned into the *Xho*I and *Not*I sites of the pPC111 expression vector (a gift of G. Kato, Johns Hopkins University), which fused a polyhistidine tag in frame to the amino terminus of the protein. This protein was expressed in *E. coli* and purified with the Xpress system (Invitrogen) as specified by the manufacturer. This fusion protein was then shipped to HRP, Inc., Denver, Pa., for the generation of polyclonal antisera from rabbits.

Subcellular localization. Cos-7 cells were plated on glass coverslips and transfected with either pHA-*rcl*, pSG5, or pSG5-*rcl* with DEAE-dextran as previously described (12). Immunofluorescence was then performed as previously described with anti-Rcl antisera and tetramethylrhodamine-5-isocyanate (TRITC)-conjugated goat anti-rabbit antibody (Hyclone) (12).

Immunoblotting. Cultured cells were washed once with phosphate-buffered saline, scraped into Western scraping buffer (40 mM Tris-HCl [pH 7.4], 1 mM EDTA [pH 8], 150 mM NaCl), and lysed in 10% SDS. Relative protein amounts were determined with the bicinchoninic acid kit (Pierce, Rockford, Ill.). Equal amounts of protein were loaded per lane and run on SDS-polyacrylamide gels. Immunoblotting was then performed, as previously described, by enhanced chemiluminescence (Amersham, Arlington Heights, Ill.) (26). c-Myc protein was detected with the 9E10 monoclonal antibody at a 1:2,000 dilution (16). The HA-tagged protein was detected with monoclonal antibody 12CA5 at a 1:1,000 dilution. The rabbit polyclonal anti-Rcl antibody was used at a 1:1,250 dilution.

Soft agar assays. A total of 1.2×10^5 cells of either Rat1a, Rat1a-myc, Rat1a-pSG5, or Rat1a-rcl in twofold-concentrated DMEM–20% fetal bovine serum were mixed with an equal volume of 0.8% agarose and poured onto a bed of 0.7% agarose as previously described (27). The cells were fed every 3 days with 2 ml of DMEM–10% fetal bovine serum. After 12 to 14 days, photomicrographs were taken and colonies were counted. The experiments were repeated three times.

Apoptosis assays. A total of 5×10^5 cells from the above cell lines were plated in DMEM–10% fetal bovine serum and allowed to grow overnight. The cells were then washed once with phosphate-buffered saline, refed with medium containing either 10 or 0.1% fetal bovine serum, and incubated for 24 h as previously described (26). Photomicrographs were then taken.

Nucleotide sequence accession numbers. The nucleotide sequence accession numbers in the GenBank database are U82591 for *rcl* cDNA and U83666 for the rat BUB1 amplicon.

RESULTS

Effect of c-Myc expression on nonadherent fibroblasts. We sought to identify genes that act downstream of c-Myc in Rat1a fibroblasts, which can be transformed in a single step through exogenous c-Myc expression (54, 56). In contrast to Rat1a cells, Rat1a-myc cells are able to form colonies in soft agar (anchorage-independent growth) (Fig. 1A) (27, 56). This phenotype provides a model that closely mimics tumor growth in vivo and a unique experimental opportunity to identify the genetic program underlying Myc-mediated anchorage-independent growth. Rat1a-myc cells also undergo apoptosis when cultured at low serum concentrations (Fig. 1A) (17, 26, 42). We examined the differences in gene expression between nonadherent Rat1a and Rat1a-myc cells to identify genes that confer the anchorage-independent growth phenotype of Rat1a-myc cells.

To place the c-Myc-responsive genes in the context of the

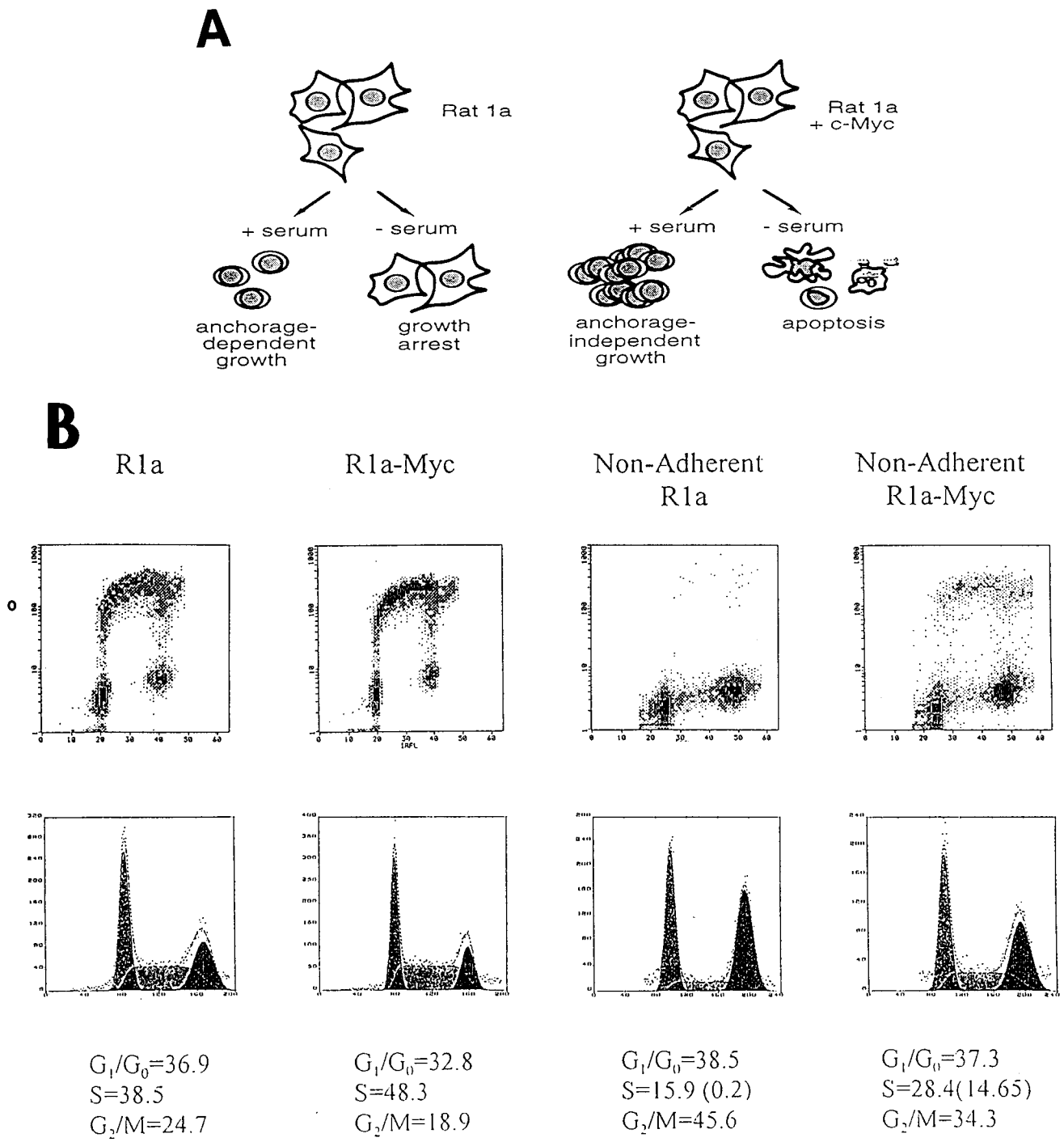

FIG. 1. (A) Schematic of the phenotypic characteristics of Rat1a cells and Rat1a cells expressing ectopic human c-Myc (Rat1a-myc). (B) Cell cycle distribution of and BrdU incorporation in adherent and nonadherent Rat1a and Rat1a-myc cells. Two-dimensional flow-cytometric distributions of DNA content determined by propidium iodide staining (abscissa) and DNA synthesis determined by BrdU labeling (ordinate) are shown for each cell line. Distributions of nuclei in each cell cycle compartment were estimated by deconvolution of propidium iodide staining profiles. The numbers in parentheses indicate the percentage of cells in S phase (by DNA content) actively incorporating BrdU.

cell cycle, we determined the cell cycle distribution and DNA-synthetic capability (BrdU incorporation) of Rat1a and Rat1a-myc cells grown either adherently or nonadherently (Fig. 1B). A higher percentage of Rat1a-myc cells (48.3%) than of Rat1a cells (38.5%) were in S phase and incorporated BrdU. When the cells were cultured nonadherently for 48 h, their cell cycle profiles appeared dramatically different. The percentage of Rat1a cells in G_1 was only slightly increased. However, there was a decrease in the percentage of cells in S phase (to 15.9%) with an equal increase in the percentage of cells in G_2/M (45.6%) (Fig. 1). Rat1a-myc cells showed a slight increase in the percentage of cells in G_1 and an increase in the percentage

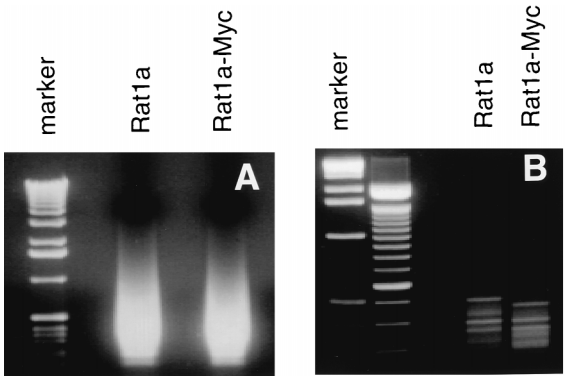

FIG. 2. Ethidium bromide-stained agarose gels showing amplicons generated from Rat1a and Rat1a-myc cells (A) and differential amplicons after two rounds of RDA with Rat1a amplicons as the tester and Rat1a-myc amplicons as the driver (Rat1a) or Rat1a-myc amplicons as the tester and Rat1a amplicons as the driver (Rat1a-myc) (B). The marker represents a 1-kb ladder (GIBCO-BRL). The unlabelled lane in panel B is a 100-bp ladder size marker (GIBCO-BRL).

of cells in G_2/M, with a concomitant decrease in the percentage of S-phase cells (Fig. 1B). When the ability of the nonadherent cells to incorporate BrdU into their DNA was assayed, the Rat1a cells in S phase were found to incorporate BrdU less efficiently, suggesting that these cells are incapable of DNA synthesis (Fig. 1B). The majority of Rat1a-myc cells in S phase were able to incorporate BrdU, demonstrating their retained capacity to undergo DNA synthesis (Fig. 1B).

cDNA RDA. We cultured Rat1a and Rat1a-myc cells for 48 h on dishes that had been coated with a layer of agarose so that the cells were unable to adhere. Poly(A)$^+$ RNA was harvested and used to synthesize cDNA. These cDNAs were then prepared for amplification and subsequently for RDA, as outlined in Materials and Methods. After two rounds of RDA, we were able to view several distinct PCR fragments that were unique to either Rat1a or Rat1a-myc cells. A typical ethidium bromide-stained agarose gel of the PCR fragments after two rounds of RDA with either Rat1a or Rat1a-myc as the "tester" is shown (Fig. 2).

The PCR products were isolated and analyzed to determine whether they represented differentially expressed genes (Fig. 3A). Unique PCR fragments were subcloned into either pBluescript KS (Stratagene) or PCR 2.1 (Invitrogen). We first used a rapid screen to determine if the cloned cDNA fragments were represented in different amounts in pools of PCR-amplified cDNA fragments (amplicons) generated from either Rat1a or Rat1a-Myc cells. Clones with small size differences, usually derived from an apparent single band, were ^{32}P labeled and hybridized to Southern slot blots of Rat1a and Rat1a-myc amplicons. Two representative clones are shown in Fig. 3B. The introduction of this step into the RDA procedure allowed us to screen the many subclones derived from a single band without using limiting resources such as poly(A)$^+$ RNA. In our experience, a single band contained as many as three independent cDNA fragments as identified by restriction enzyme digestion and sequence analysis. Subclones that appeared to be differentially represented by slot blot analysis, termed differential amplicons, were then tested for differential expression by either an RNase protection assay or Northern blot analysis (Fig. 3C). Of 23 differential amplicons analyzed, 21 (representing 20 cDNAs) were differentially expressed. The names of the differential amplicons identified in this screen and their corresponding genes, as identified by BLAST homology searches,

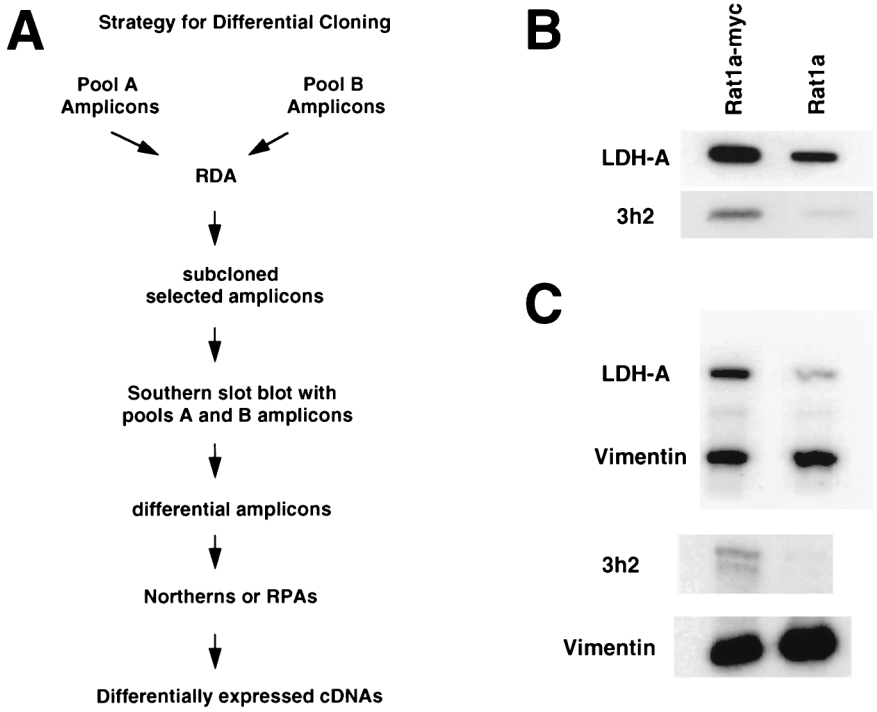

FIG. 3. (A) Outline of the strategy and terminology used to identify differentially expressed cDNAs between Rat1a and Rat1a-myc cells. (B) Slot blot hybridization of two representative selected amplicons demonstrating differential representation between Rat1a and Rat1a-myc amplicons. (C) RNase protection assays demonstrating differential mRNA expression of LDH A (upper panel) and 3h2 (lower panel). Vimentin, which is not differentially expressed in this system, is used as a control in both experiments.

TABLE 1. Differential amplicons identified by RDA

RDA expt no.	Clone	Size (bp)	Differential mRNA	Fold change	Sequence
1 (two cycles)	m2b4	260	Yes	Up 8×	Rcl
	m47	450	Yes	Up 3×	Unmatched
	m2b5	250	Yes	Up 7×	α-Tubulin
	m2a9	220	No	None	Vimentin
2 (two cycles)	hs8	140	Yes	ND[a]	Collagen α1 type (III)
3 (two cycles)	hsg6	550	Yes	ND	Mitochondrial cytochrome *c* oxidase
	hsd4	500	Yes	ND	Collagen α2 type (V)
	hsa3	720	Yes	Down 4×	Mss4 (Sec4)
	hsj3	320	Yes	Up 4×	Human Myc
	hsc12	420	Yes	ND	α-Tubulin
	hsi4	380	Yes	Up 6×	Mer 5
	hsh5	400	Yes	Up 3×	Unmatched
4 (three cycles)	3b2	560	Yes	Down 3×	Fibronectin
	3h3	620	Yes	ND	ODC
	3d3	430	Yes	Up 2×	EST 86E11
	3f4	340	Yes	Up 5×	EST HIBR12
	3h2	550	Yes	Up 20×	EST H59390
	3i3	520	Yes	Up 5×	BUB1
	3j7	530	Yes	Up 3×	Chaperonin
	3m5	360	Yes	Up 6×	LDH-A
	3n12	250	Yes	Up 3×	Kinesin related
	3n6	320	No	None	Fatty acyl-CoA[b] synthetase
	3l6	400	Yes	Up 3×	Ferritin heavy chain

[a] ND, not determined.
[b] CoA, coenzyme A.

are listed in Table 1. Included in this list is the human c-*myc* amplicon that was isolated from Rat1a-Myc cells, providing evidence that we were able to identify differentially expressed cDNAs by this system.

Among the cDNAs found to be upregulated by c-Myc were those encoding ODC, a previously established target of c-Myc (2, 3, 43, 59), and lactate dehydrogenase A (LDH A), recently shown to be upregulated by c-Myc (54, 58), strongly suggesting that the other members of this group represented differentially expressed genes responsive to c-Myc. Among the cDNAs downregulated by c-*myc* were two collagen genes, which were previously shown to be downregulated by c-Myc (58, 60). Conspicuously absent from the list in Table 1 were the cDNAs for cyclin A, prothymosin α, and CDC 25A, all of which are thought to act downstream of c-Myc (1, 15, 18, 25, 29, 44). Their absence and the absence of amplicon fragments appearing multiple times suggest that our screen was not saturating. Of the 20 differentially expressed cDNAs, five were novel or matched only to expressed sequence tag (EST) sequences by BLAST search homology. One of the unknown cDNA fragments, M2B4, hereafter referred to as *rcl*, was chosen for further study because of its marked differential expression in nonadherent Rat1a-myc and Rat1a cells.

Characterization of *rcl*, a novel c-Myc-responsive gene. By Northern analysis, the *rcl* probe hybridized to bands of 900 and 600 bp, suggesting the existence of family members or the generation of different RNA species from the same gene (Fig. 4A). The mRNA species hybridizing to the *rcl* fragment were present at greater than eightfold-higher levels in nonadherent Rat1a-myc cells than in nonadherent Rat1a cells (Fig. 4A). We examined the expression of these mRNAs in attached and unattached Rat1a and Rat1a-myc cells to determine if their expression was dependent on adherence to the extracellular matrix. RNase protection assays were performed with total RNA isolated from either attached or unattached Rat1a and Rat1a-myc fibroblasts. *rcl* showed approximately a twofold increase in attached Rat1a-myc cells compared to attached Rat1a cells but an eightfold difference when these cells were unattached (Fig. 4B). Interestingly, attached Rat1a cells expressed *rcl* at approximately 30-fold-higher levels than did unattached Rat1a cells, suggesting that *rcl* expression may be

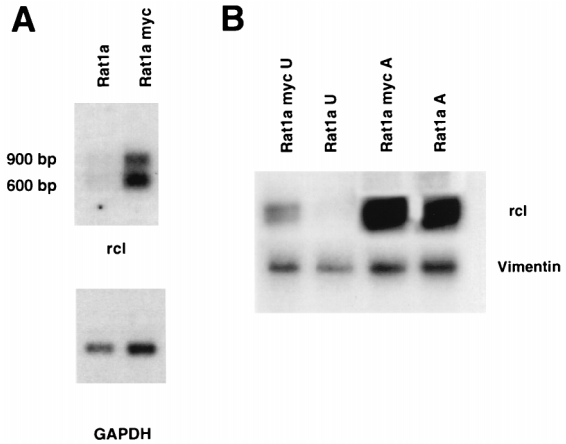

FIG. 4. (A) Northern blot demonstrating differential expression of *rcl* between nonadherent Rat1a and Rat1a-myc cells. Glyceraldehyde-3-phosphate dehydrogenase (GAPDH) (lower panel) is used as a control. (B) RNase protection assay demonstrating the adhesion dependence of *rcl* expression. A 10-μg portion of total RNA from either adherent (A) or nonadherent (U) cells was used. Vimentin was used as a control.

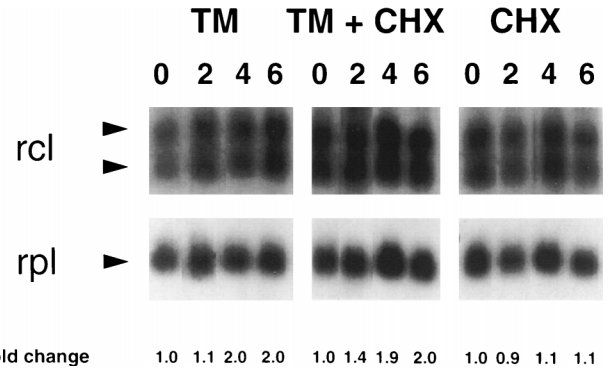

FIG. 5. Northern blot demonstrating *rcl* mRNA induction by the Myc-ER system. A 15-μg portion of total RNA from Rat1a Myc-ER cells at various hours (at top of lane) after treatment with 4-hydroxytamoxifen (TM; 0.25 μM), 4-hydroxytamoxifen and cycloheximide (TM+CHX; 0.25 μM), or cycloheximide (CHX; 10 μM) were hybridized to the *rcl* cDNA fragment. The ribosomal protein rpL32 cDNA was used as a control.

regulated in part by signals from the extracellular matrix (Fig. 4B).

To determine whether *rcl* is a direct target of c-Myc, we used the chimeric Myc-ER system, in which Myc activity is switched on by exposure of cells stably expressing Myc-ER to tamoxifen (14). When the liganded Myc-ER fusion is switched on, genes downstream of c-Myc are activated. Direct target genes are activated by the Myc-ER fusion in the presence of cycloheximide, which prevents any intermediate steps that require protein synthesis. In three independent experiments, we observed that the level of *rcl* mRNA was increased twofold by exposure of Myc-ER-transfected Rat1a cells to tamoxifen or to tamoxifen plus cycloheximide (Fig. 5). By contrast, exposure to cycloheximide alone did not increase *rcl* expression. It is notable that the expression of ODC was induced only 1.5-fold in this system (data not shown). These observations suggest that *rcl* is directly regulated by c-Myc.

An oligo(dT)-primed rat liver cDNA library (Stratagene) was screened with the 260-bp *rcl* cDNA fragment as a probe, since *rcl* expression was seen to be high in the liver (see Fig. 10A). Three cDNAs (designated C4, C5, and C6) of 548, 564, and 730 bp were identified. Analysis of the open reading frames of the cDNAs showed that the coding sequence was the same for all three cDNAs. C4 and C5 were identical, with C5 sequence extending 16 bp further 5′. The C6 sequence did not contain the 5′ 40 nucleotides and extended 240 nucleotides downstream before ending. Furthermore, the C5 and C6 cDNAs shared an imperfect polyadenylation signal (AAGAAA) 12 nucleotides upstream from the poly(A) tail of C5, while C6 had another polyadenylation signal further downstream, suggesting that C5 and C6 were generated by the use of alternate polyadenylation signals. This provides an explanation for the sizes of the two hybridizing mRNA species identified by Northern blot analysis (Fig. 4A).

Sequence analysis of the C5 cDNA clone revealed a Kozak consensus sequence (GCGATGG) close to the 5′ end of the cDNA in frame with the longest open reading frame of the cDNA. Translation in this reading frame predicts a 163-amino-acid protein. Following in vitro transcription and translation of the C5 cDNA a doublet of 23 and 27 kDa was seen (data not shown). Analysis of the Rcl amino acid sequence showed no known functional motifs or domains. Computer analysis predicted the protein to be highly alpha-helical with the potential for coiled-coil interactions. The presence of several evenly spaced leucines that are conserved across the rat, mouse, and human sequences suggests that this might be the case (Fig. 6). We have recently demonstrated that Rcl can homodimerize in the yeast two-hybrid system (34). The protein also has three cysteines, two of which are clustered toward the N terminus, suggesting the possibility for intra- and intermolecular disulfide or metal ion linkages. The protein also contains a potential nuclear targeting sequence (Fig. 6).

A search of the database found a mouse EST expressed in the F9 embryonal carcinoma cell line, and human ESTs from the Merck/Washington University project that appeared to represent the human homolog of *rcl*. We have obtained, characterized, and sequenced the human EST clone (IMAGE Consortium clone 298414). Translation and alignment of the ESTs with Rcl showed 90% identity and 94% conservation between rat Rcl and the ESTs at the amino acid level and 84% identity and 93% conservation between rat Rcl and human ESTs over

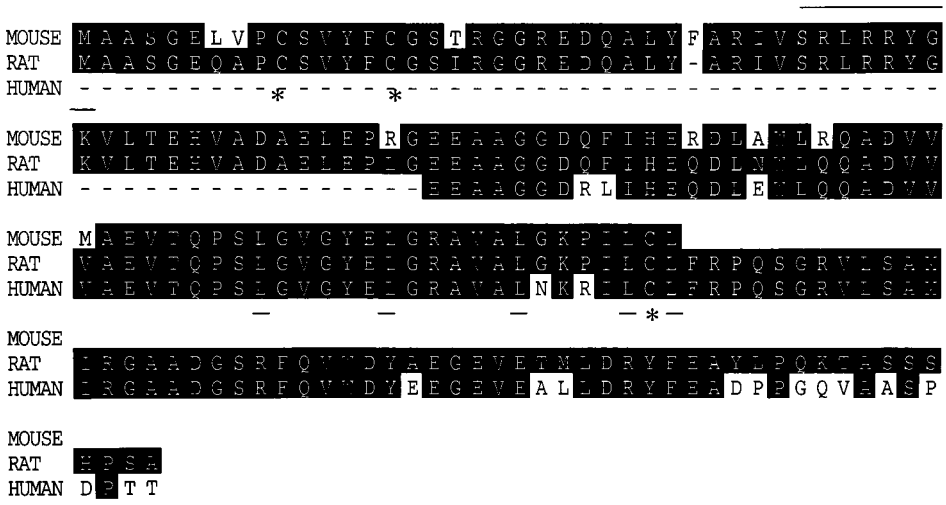

FIG. 6. Amino acid sequence alignment demonstrating a high degree of conservation of the Rcl protein sequence between rat, mouse, and human. Conserved residues are shaded in black. The putative nuclear targeting sequence is overlined, and key conserved leucine (underline) and cysteine (*) residues are shown. Alignment was generated with the DNAStar computer program.

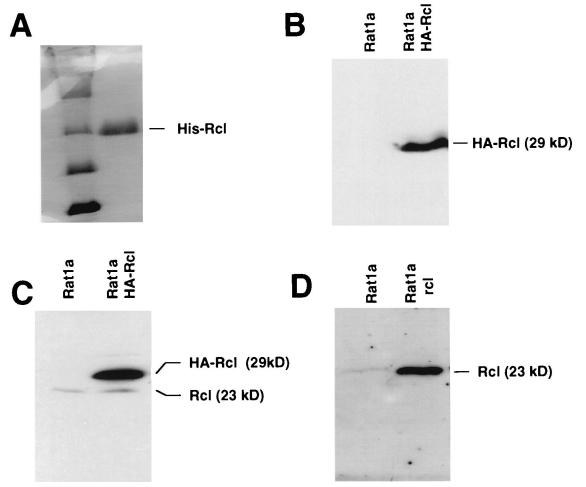

FIG. 7. (A) Coomassie blue-stained gel of His-tagged Rcl after purification by the Xpress system (Invitrogen), demonstrating the purity of the antigen used in antibody production. The left lane shows molecular mass standards (from bottom, 14.4, 21, 31, and 45 kDa). (B and C) Identification by immunoblotting of the 29-kDa HA-tagged Rcl in transfected Rat1a cells with the anti-HA monoclonal 12CA5 antibody (B) and anti-Rcl polyclonal antiserum (C). (C) Identification of endogenous 23-kDa Rcl by immunoblotting with anti-Rcl antiserum. (D) Demonstration of high levels of Rcl expression in transfected Rat1a cells by immunoblotting with anti-Rcl antiserum.

an extended region of 94 amino acids, although their sequences diverge at the C-terminal 13 amino acids (Fig. 6).

Characterization of Rcl protein. To study the expression of Rcl protein, we generated antibodies directed against a recombinant hexahistidine-tagged Rcl protein. The fusion protein was expressed in bacteria and affinity purified over a nickel column with the Xpress system (Invitrogen) (Fig. 7A). This fusion protein was used for the generation of polyclonal antisera from rabbits. The specificity of the antisera was tested by immunoblotting, first against protein lysates of Rat1a cells and HA-Rcl cells, Rat1a cells stably transfected with a construct expressing an HA-tagged Rcl protein (Fig. 7C). Using either the anti-Rcl or anti-HA 12CA5 antibody, a polypeptide of approximately 29 kDa was detected in the HA-Rcl protein lysate that was absent in the Rat1a lysate, indicating that this was the HA-Rcl protein (Fig. 7B and C). Also, a band of approximately 23 kDa, the size of the in vitro translation product, was seen in both lanes with the anti-Rcl antiserum, suggesting that this might represent the endogenous Rcl protein (Fig. 7C). That this 23-kDa band represented the endogenous protein was confirmed by the expression of untagged Rcl from the pSG5 expression plasmid and subsequent immunoblotting with the Rcl antisera (Fig. 7D).

We used the antisera to study the subcellular localization of Rcl. Cos-7 cells were transfected with the pSG5-rcl construct. Cells transfected with the expression construct showed bright nuclear staining, often excluding nucleoli, with low background cytoplasmic staining (Fig. 8). Untransfected cells and Cos-7 cells transfected with pSG5 showed uniform, low background staining (Fig. 8). Similar results were obtained when Cos-7 cells were transfected with the HA-Rcl construct and stained with the 12CA5 antibody specific for the HA tag (Fig. 8). These results indicate that Rcl is a 23-kDa nuclear protein.

Correlation between c-*myc* and *rcl* expression. Having determined that c-Myc can directly stimulate *rcl* mRNA expression in Rat1a cells, we sought to determine whether the induction of c-Myc expression could lead to induction of Rcl protein expression. We used a Rat1a MT-myc cell line in which c-*myc* expression is regulated by a sheep metallothionein promoter (26). The addition of Zn^{2+} induces c-*myc* expression and results in anchorage-independent growth (data not shown). Rat1a MT-myc cells were allowed to grow to confluence in regular growth medium. c-Myc expression was then induced by the exposure of cells to $ZnSO_4$. c-Myc protein expression was

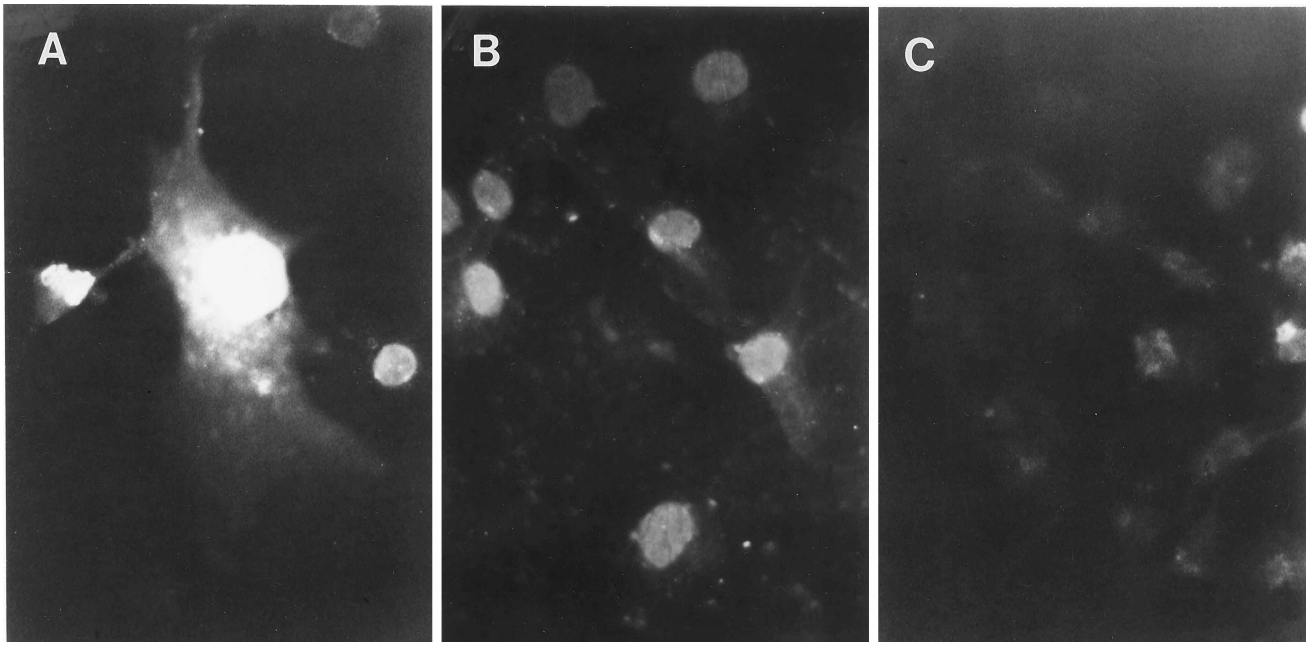

FIG. 8. Immunofluorescence of Cos-7 cells transfected with the pSG5-*rcl* (A), HA-Rcl (B), and vector (C), demonstrating nuclear localization of Rcl. Transfected cells were stained with either anti-Rcl antiserum (left panel) or anti-HA monoclonal antibody (middle and right panels) followed by appropriate TRITC-conjugated secondary antibody.

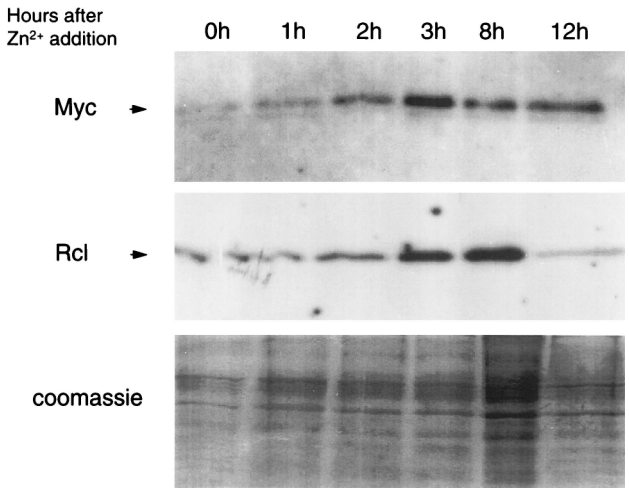

FIG. 9. Induction of Rcl protein expression by stimulating c-Myc expression. Rat1a cells stably transfected with a zinc-inducible MT-Myc plasmid were grown to confluence, and then 50 μM zinc sulfate was added to the medium to stimulate c-Myc expression. Cell lysates collected at the indicated time points were tested by immunoblotting for c-Myc (with a 9E10 anti-Myc monoclonal antibody) and Rcl expression (with anti-Rcl antiserum). The bottom panel shows a Coomassie blue-stained gel of cells lysates used for immunoblots shown in the upper panels.

induced as rapidly as 1 h and peaked at 3 h after $ZnSO_4$ addition (Fig. 9). Rcl expression increased after 3 h in Zn^{2+}, peaked at 6 to 8 h after the addition of zinc, and then declined at 12 h (Fig. 9). These observations suggest, in addition to elevation of *rcl* mRNA levels, that c-Myc stimulates Rcl protein expression.

To establish further the link between c-Myc and *rcl* expression, we examined the tissue expression pattern of *rcl* and c-*myc*. An RNase protection assay with both *rcl* and c-*myc* RNA probes (Fig. 10A) revealed that the tissue expression patterns of c-*myc* and *rcl* were very similar, with the exception of low c-*myc* expression in the adult liver. Our observations correlate well with previous reports of the expression pattern of c-*myc* mRNA in adult mouse tissues and further suggest that the expression of *rcl* may be related to or influenced by c-*myc* expression (51, 61). We also observed a correlation between c-Myc expression and levels of *rcl* mRNA, which appear as a single 750-bp broad band (Fig. 10B), in human lymphoid cells. CB33 is an immortalized nontransformed human lymphoblastoid cell line. c-*myc*-transformed CB33-myc cells and three human Burkitt's lymphoma cell lines all demonstrate elevated *rcl* mRNA levels (Fig. 10B). These observations provide support for the regulation of *rcl* by c-Myc.

Since *rcl* was cloned in a system in which enforced c-Myc expression conferred a growth capability (anchorage independence) to Rat1a cells, we sought to determine whether *rcl* expression could be induced in an in vivo growth system. At various time points after partial hepatectomy, which is known to induce peak c-*myc* expression at 3 to 4 h, RNA samples taken from regenerating rat livers were analyzed for *rcl* expression levels by RNase protection assays. *rcl* expression was shown to be induced as early as 6 h after partial hepatectomy and continued to increase through 12 to 24 h (Fig. 10C). In addition, *rcl* expression in serum-starved Rat1a cells was induced after 6 h of reexposure to serum (data not shown). These data further suggest that *rcl* expression is associated with in vitro and in vivo cell proliferation.

Biological activity of *rcl*. We examined the role of *rcl* in c-Myc mediated phenotypes with specific reference to anchorage-independent growth. We created stable cell lines in Rat1a

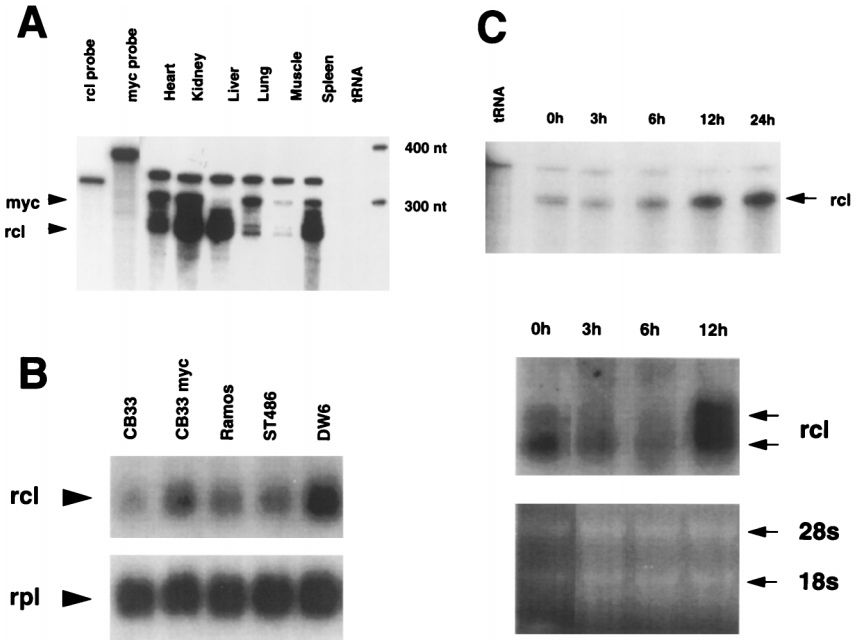

FIG. 10. (A) RNase protection assay showing the tissue distribution pattern of c-*myc* and *rcl* expression. A 10-μg portion of total RNA was incubated simultaneously with c-*myc* and *rcl* probes. Undigested *rcl* and *myc* probes are shown in the first two lanes on the left. tRNA control and RNA size markers are shown in the last two lanes. RNA products were resolved on an acrylamide-urea gel. (B) Expression of *rcl* mRNA is elevated in human lymphoblastoid (CB33-myc) or Burkitt's lymphoma (Ramos, ST486, and DW6) cells overexpressing c-*myc*. A 15-μg portion of total RNA per lane is shown. A human *rcl* cDNA was used as a probe, and rpl32 was used as a control. (C) RNA assays showing *rcl* expression levels in regenerating rat liver. RNA isolated from regenerating livers at the indicated time points after partial hepatectomy were subjected to an RNase protection assay with an rcl probe (top panel). Total RNA samples (20 μg/lane) from regenerating rat livers were also analyzed by Northern blotting for *rcl* expression; the bottom panel shows the ethidium bromide-stained agarose gel.

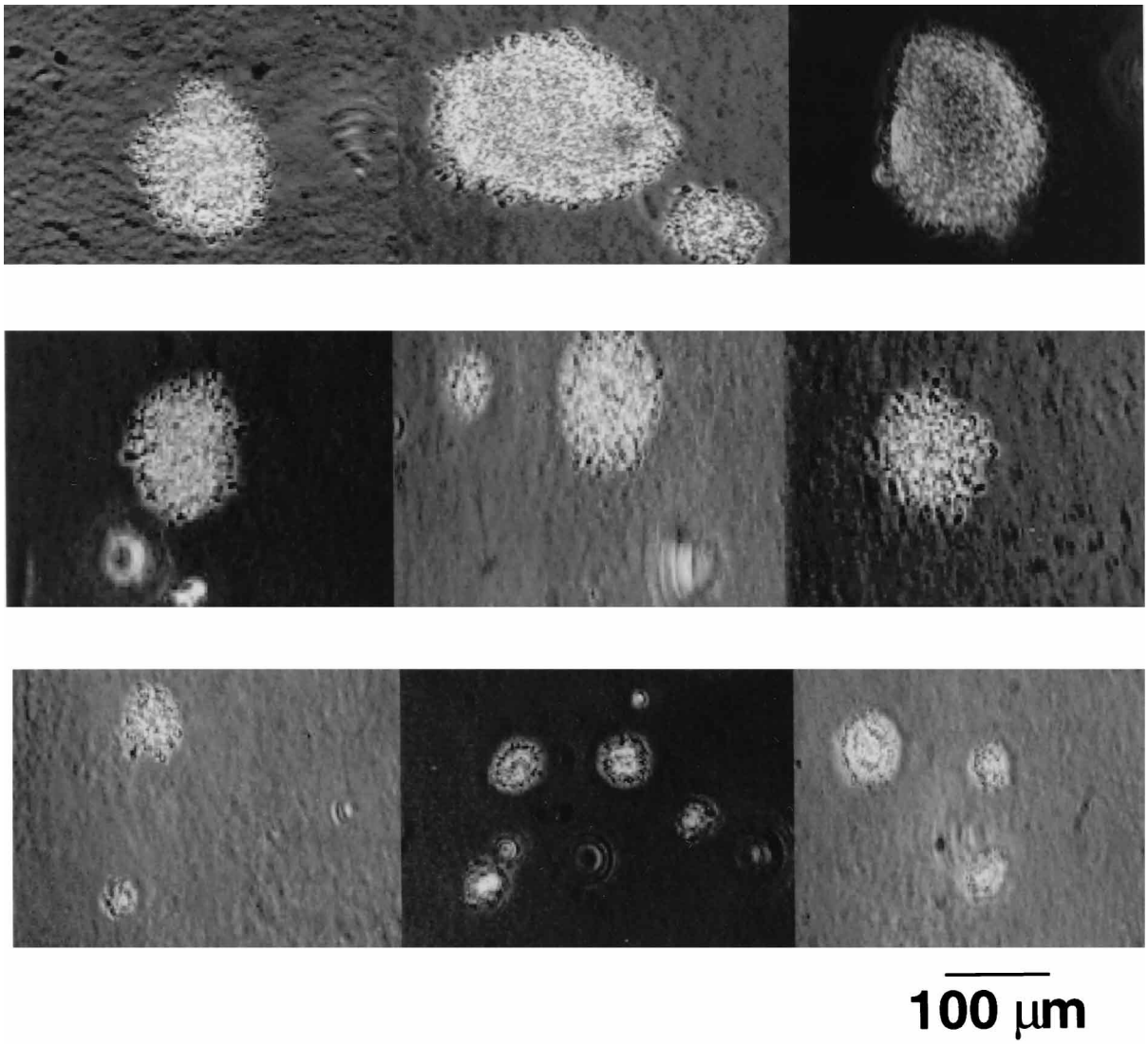

FIG. 11. Induction of anchorage-independent growth by *rcl*. Pools of Rat1a cells stably transfected with either c-*myc* (top row), *rcl* (middle row), or pSG5 (bottom row) were plated in soft agarose, and photomicrographs of representative colonies were taken after 2 weeks. The number of colonies with diameters greater than 100 μm was counted in five experiments. Rat1a-*rcl* cells displayed 930 ± 270 colonies per 100-mm dish (cloning efficiency, 0.0078), and Rat1a-myc displayed 7,600 ± 1,020 colonies per 100-mm dish (cloning efficiency, 0.063).

cells which constitutively expressed high levels of Rcl protein. Pools of puromycin-resistant colonies, which express high levels of Rcl by immunoblot (Fig. 7D), were tested in soft agar growth assays. Rat1a-*rcl* cells displayed anchorage-independent growth and consistently formed larger colonies in the soft agar assays than did the empty vector control or parental Rat1a cells (Fig. 11). These observations suggest that Rcl overexpression is sufficient to cause anchorage-independent growth in Rat1a cells, although the colonies were on average half the diameter of those created by Rat1a-myc cells and the cloning efficiency was eightfold lower than in Rat1a-myc cells (Fig. 11).

Since overexpression of c-Myc induces apoptosis of serum-starved Rat1a cells, we tested whether Rat1a-*rcl* cells will undergo apoptosis under serum-deprived conditions. Cells were plated in DMEM containing 10% fetal calf serum and then exposed for 24 h to medium containing 0.1% fetal calf serum. Rat1a-myc cells showed high levels of apoptosis as previously described (26). Neither the Rat1a-*rcl* cells nor the Rat1a-pSG5 cells showed significant apoptosis (data not shown). These observations suggest that Rcl expression is not sufficient to induce apoptosis in Rat1a cells. Further, these data suggest that c-Myc may stimulate anchorage-independent growth and apoptosis through separate pathways.

DISCUSSION

We developed a strategy to exploit a unique biological system to examine the genetic program activated by c-Myc in the transformation of Rat1a fibroblasts. Our experimental approach was designed to identify genes that are differentially expressed in nonadherent Rat 1a-myc cells and Rat 1a cells. This strategy directly examines the genetic events that may link c-Myc expression to the transformed phenotype.

To place the differentially expressed genes in a biological context, we first studied the differences in the cell cycle profiles of nonadherent Rat1a and Rat1a-myc cells. In contrast to

previous perceptions that nonadherent cells are primarily arrested in the G_1 phase of the cell cycle, we unexpectedly observed both G_1 and G_2/M blocks in unsynchronized nonadherent Rat1a cells (23, 24). These blocks appear to be abrogated by overexpression of c-Myc in the nonadherent Rat1a cells.

Using representational difference analysis, we identified 17 upregulated genes and 3 downregulated genes linked to c-Myc overexpression. It is possible that some of these genes were indirectly affected by c-Myc and that their elevated expression merely reflected the proliferative status of the nonadherent Myc-transformed Rat1a cells. Notwithstanding this caveat, this collection of genes includes known growth-related genes such as that encoding ODC, which has been previously shown to be upregulated by c-Myc (2, 3, 43, 59), as well as several collagen genes, some of which are downregulated by c-Myc (58, 60). Five of the upregulated genes are either unknown or match only with EST sequences available in the databases.

Overexpression of c-Myc in Rat1a-myc cells allows the nonadherent cells to undergo DNA synthesis and progress through the cell cycle. Intriguingly, two of the differentially expressed cDNAs identified in our study, the ODC and LDH A genes, have been shown to affect DNA replication (22, 53). The accumulation of nonadherent Rat1a cells in G_2/M and the ability of Rat1a-myc cells to overcome this block suggest that c-Myc may play a role in the G_2/M transition as well as in the G_1/S transition. It has been previously reported that c-Myc transcription activation activity is maintained in G_2/M (52). Intriguingly, one novel clone, 3i3, encodes a stretch of amino acids homologous to the yeast BUB1 gene product that is known to regulate the G_2/M spindle checkpoint (46). Taken together, these data suggest a critical role for c-Myc in several stages of the cell cycle and suggest that the anchorage-independent growth phenotype caused by the enforced expression of c-Myc in Rat1a fibroblasts is a result of the perturbation of normal controls at several points along the cell cycle and is not restricted to G_1.

We selected and studied one of the novel cDNAs identified by RDA, which we have termed *rcl*. *rcl* encodes a 23-kDa nuclear protein of unknown function. The *rcl* and c-*myc* mRNA expression patterns are similar in adult rat tissues. Activation of the Myc-ER fusion by tamoxifen in the presence of cycloheximide increases *rcl* expression. In addition, Rcl protein expression can be stimulated by induction of c-Myc expression in confluent Rat1a fibroblasts, confirming its role as a downstream effector of c-Myc. *rcl* expression appears to closely parallel cell proliferation in different models. Its expression is stimulated in a system of regenerating rat liver and is elevated in human lymphoblastoid or lymphoma cells overexpressing c-Myc.

Identification of putative c-Myc-responsive genes. Rat1a and Rat1a-myc cells show no significant phenotypic differences when cultured adherently in serum-containing media (1). However, Rat1a cells are not capable of anchorage-independent growth whereas Rat1a-myc cells are, as demonstrated in soft-agar assays (27, 56). We therefore hypothesized that there exists a genetic program which is induced by constitutive c-*myc* expression in nonadherent Rat1a-myc cells that is either shut off or downregulated in Rat1a cells. We further hypothesized that genes that are differentially expressed between Rat1a-myc cells and Rat1a cells grown under nonadherent conditions contribute to the anchorage-independent growth phenotype of Rat1a-myc cells. We have previously shown that cyclin A is differentially expressed in this system and that expression of exogenous cyclin A is able to confer anchorage-independent growth to Rat1a cells (1). In this previous study, we also showed that not all growth-related genes are differentially expressed in this system. Neither cyclin D or cyclin E protein levels were significantly altered between the two cell lines. These data suggested that the differentially expressed genes are regulated by c-Myc expression and contribute to the anchorage-independent growth phenotype of Rat1a-myc cells. We therefore set out to identify other genes involved in this process.

We applied cDNA RDA to cDNAs generated from nonadherent Rat1a and Rat1a-myc cells which constitutively express human c-*myc*. Our goal was to identify the genes that play roles in the transformation phenotype of anchorage-independent growth induced in Rat1a cells by enforced c-Myc expression. We used Rat1a-myc cells rather than an inducible cell line because Rat1a-myc cells represent deregulated c-Myc expression and therefore more closely mimic the case of human tumors in which deregulated c-Myc expression is found. Applying cDNA RDA to these cells, we identified 23 differently represented cDNA fragments. Of these, 21, representing 20 cDNAs, were shown to be differentially expressed, by either Northern blot analysis or RNase protection assays.

In our RDA strategy, we introduced the use of slot blot hybridization as an initial test for differential amplicons. We surmise that the introduction of this step into the RDA procedure increased its sensitivity. We were therefore able to identify a series of cDNAs that, by Northern blot analysis or RNase protection assays, were differentially expressed at levels ranging from 2- to 20-fold, indicating the great sensitivity of this assay. The low false-positive rate (21 of 23 differential amplicons represented differentially expressed cDNAs) is similar to that found by others, compares favorably with that of other methods of detecting differential gene expression such as differential display, and demonstrates the efficacy with which RDA identifies differentially expressed cDNAs (7, 28, 36).

Among the cDNAs identified in our screen, only the α-tubulin gene was represented more than once by differential amplicons. This cDNA was represented by two amplicons that represented different segments of the cDNA. No amplicon was represented more than once, suggesting that our screen was not saturating. This is confirmed by the absence of the prothymosin α, CDC 25A, and cyclin A genes, all of which have been shown to be c-*myc*-responsive genes, although the prothymosin gene has not been implicated in c-*myc* phenotypes, and its differential expression in this system has not been assayed (1, 15, 18, 29). This is in contrast to the experience of Braun et al. (7), who identified several *EWS/FLI1* upregulated amplicons on multiple occasions, and demonstrates that deregulated c-Myc expression alters the expression of a large number of genes, underscoring the importance of c-Myc as a key regulator of cell proliferation.

While previous studies have identified individual genes or groups of genes that appear to be c-Myc responsive, none have used conditions under which c-Myc phenotypes are manifested (2, 3, 5, 15, 39, 40, 58). Thus, the collection of differentially expressed cDNAs identified in this study sheds considerable light on how c-Myc confers anchorage-independent growth capability to Rat1a cells and contributes to tumorigenicity in vivo. LDH A mRNA expression was previously shown to be stimulated by c-Myc (58). We have recently demonstrated that *LDH-A* expression is stimulated directly by c-Myc in an E-box-dependent manner, that LDH-A is necessary for anchorage-independent growth in several cell lines, and that LDH A is involved in other c-Myc phenotypes (54). The reasons for c-Myc regulation of other known genes identified in this study may similarly become clear.

The identification of several fragments representing novel cDNAs provides an unique opportunity to gather further in-

sight into how c-*myc* mediates its effects in cell transformation in vitro and in humans. We have begun analysis of expression levels of several of the cDNAs identified in this screen in human lymphoma cell lines and other solid-tumor cell lines. Characterization of these novel cDNAs may lead to greater understanding of the many complex events that occur downstream of c-Myc.

Cloning of *rcl*, a novel growth-related gene. Several of the differential amplicons identified in our screen were shown to be novel by BLAST homology searches. We chose one of these differential amplicons, *rcl*, for further analysis. By Northern blot analysis, *rcl* was shown to hybridize to two bands of approximately 600 and 900 nucleotides. These mRNAs were present at greater than eightfold-higher levels in nonadherent Rat1a-myc cells than in nonadherent Rat1a cells. RNase protection assays on RNA from adherent and nonadherent Rat1a and Rat1a-myc cells demonstrated that the expression of these mRNAs is also regulated by cell adherence to the extracellular matrix. RNA levels decreased 30-fold when Rat1a cells were made nonadherent. However, constitutive c-Myc expression allowed continued expression. Thus, the mRNA species identified by *rcl* are highly differentially expressed between nonadherent Rat1a and Rat1a-myc cells, and their expression is enforced by constitutive c-Myc expression, as we hypothesized.

Examination of the tissue expression of *rcl* mRNA showed that *rcl* was most highly expressed in the kidney, liver, and spleen, with very low expression in skeletal muscle. This expression pattern closely correlates with that of c-*myc* in adult tissues. Furthermore, our observation of a link between elevated c-Myc and elevated *rcl* mRNA levels in human lymphoid cells further supports the hypothesis that *rcl* is a c-Myc-responsive gene.

Our studies with the Myc-ER fusion protein suggest that *rcl* is directly activated by c-Myc. Moreover, induction of c-Myc expression from a metallothionein promoter in confluent fibroblasts led to rapid induction of Myc at 2 h after the addition of Zn^{2+}, with peak expression after 3 h. This was followed closely by a wave of Rcl expression, with an increase after 3 h and a peak after 6 to 8 h. These data demonstrate that c-Myc is able to induce Rcl expression, even in confluent cells that are unable to progress through the cell cycle, confirming the regulatory role of c-Myc on *rcl*.

Since *rcl* was identified in a system in which enforced c-*myc* expression confers a growth capability (anchorage independence) to Rat1a-myc cells of which Rat1a cells are not capable, we determined if *rcl* expression was regulated in other proliferation models. When we studied *rcl* expression in the growth system of regenerating rat liver, we observed a significant increase in *rcl* mRNA levels beginning 6 h after partial hepatectomy, with a continued increase through 24 h. *rcl* expression is therefore linked to the stimulation of proliferation in cells in vivo. This demonstrates that the role of *rcl* in growth is not restricted to tissue culture phenomena.

***rcl* induces anchorage-independent growth.** We determined whether overexpression of *rcl* in Rat1a fibroblasts could reproduce any of the c-Myc induced phenotypes seen in Rat1a cells. Stable cell lines overexpressing Rcl were generated and tested in soft agar and apoptosis assays. Rat1a-*rcl* cells displayed anchorage-independent growth in soft agar assays, consistently and reproducibly forming larger colonies than the empty-vector control. However, the cloning efficiency was low and the colonies were approximately half the diameter of those formed by Rat1a-myc cells but were comparable to those formed by overexpression of the *bmi-1* oncogene in these cells (8). This suggests that *rcl* is involved in the anchorage-independent growth phenotype induced by c-Myc in Rat1a fibroblasts.

We tested the ability of these cells to undergo apoptosis when deprived of serum. Rat1a-*rcl* cells placed in 0.1% serum-containing medium for 24 h failed to undergo apoptosis, whereas Rat1a-myc cells underwent extensive apoptosis. Rcl overexpression is therefore not sufficient to induce apoptosis in these cells under serum-deprived conditions.

Our data demonstrate that cDNA RDA is a powerful method for the identification of differentially expressed genes. Our analysis of the differentially expressed genes identified in our screen suggests that we have generated an important resource for the dissection of the mechanisms by which c-Myc transforms cells and induces tumorigenesis. Our characterization of *rcl* suggests that it is a growth-related gene and may be an important mediator of c-Myc transformation phenotypes.

ACKNOWLEDGMENTS

We thank Chris Denny for introducing us to RDA and for invaluable technical assistance; Anna Mae Diehl for regenerating liver RNA samples; Se-Jin Lee for adult rat organs and for the mouse cDNA library; Kirsten Hubbard for assistance in typing the manuscript; Gurvaneet Randhawa, Eric Fearon, and Dan Wechsler for critical review of the manuscript; and members of the Dang laboratory for helpful discussions.

B.C.L. is supported by a Howard Hughes predoctoral fellowship and training grant NIGMS07814. H.S. is a fellow of the Lymphoma Research Foundation of America. C.V.D. is a Scholar of the Leukemia Society of America. This work was supported by NIH grant CA57341 to C.V.D. and by the Wilbur-Rogers Foundation.

REFERENCES

1. **Barrett, J. F., B. C. Lewis, A. T. Hoang, R. Alvarez, Jr., and C. V. Dang.** 1995. Cyclin A links c-Myc to adhesion-independent cell proliferation. J. Biol. Chem. **270:**15923–15925.
2. **Bello-Fernandez, C., and J. L. Cleveland.** 1992. c-myc transactivates the ornithine decarboxylase gene. Curr. Top. Microbiol. Immunol. **182:**445–452.
3. **Bello-Fernandez, C., G. Packham, and J. L. Cleveland.** 1993. The ornithine decarboxylase gene is a transcriptional target of c-Myc. Proc. Natl. Acad. Sci. USA **90:**7804–7808.
4. **Benvenisty, N., A. Leder, A. Kuo, and P. Leder.** 1992. An embryonically expressed gene is a target for c-Myc regulation via the c-Myc-binding sequence. Genes Dev. **6:**2513–2523.
5. **Benvenisty, N., D. M. Ornitz, G. L. Bennett, B. G. Sahagan, A. Kuo, R. D. Cardiff, and P. Leder.** 1992. Brain tumours and lymphomas in transgenic mice that carry HTLV-I LTR/c-myc and Ig/tax genes. Oncogene **7:**2399–2405.
6. **Blackwood, E. M., L. Kretzner, and R. N. Eisenman.** 1992. Myc and Max function as a nucleoprotein complex. Curr. Opin. Genet. Dev. **2:**227–235.
7. **Braun, B. S., R. Frieden, S. L. Lessnick, W. A. May, and C. T. Denny.** 1995. Identification of target genes for the Ewing's sarcoma EWS/FLI fusion protein by representational difference analysis. Mol. Cell. Biol. **15:**4623–4630.
8. **Cohen, K. J., J. S. Hanna, J. E. Prescott, and C. V. Dang.** 1996. Transformation by the bmi-1 oncoprotein correlates with its subnuclear localization but not its transcriptional suppression activity. Mol. Cell. Biol. **16:**5527–5535.
9. **Cole, M. D.** 1991. Myc meets its Max. Cell **65:**715–716.
10. **Dang, C. V.** 1991. c-myc oncoprotein function. Biochim. Biophys. Acta **1072:** 103–113.
11. **Dang, C. V., and L. A. Lee.** 1996. c-Myc function in neoplasia. Springer-Verlag, New York, N.Y.
12. **Dang, C. V., and W. M. Lee.** 1989. Nuclear and nucleolar targeting sequences of c-erb-A, c-myb, N-myc, p53, HSP70, and HIV tat proteins. J. Biol. Chem. **264:**18019–18023.
13. **Egan, S. E., B. W. Giddings, M. W. Brooks, L. Buday, A. M. Sizeland, and R. A. Weinberg.** 1993. Association of Sos Ras exchange protein with Grb2 is implicated in tyrosine kinase signal transduction and transformation. Nature **363:**45–51.
14. **Eilers, M., D. Picard, K. R. Yamamoto, and J. M. Bishop.** 1989. Chimaeras of myc oncoprotein and steroid receptors cause hormone-dependent transformation of cells. Nature **340:**66–68.
15. **Eilers, M., S. Schirm, and J. M. Bishop.** 1991. The MYC protein activates transcription of the alpha-prothymosin gene. EMBO J. **10:**133–141.
16. **Evan, G. I., G. K. Lewis, G. Ramsay, and J. M. Bishop.** 1985. Isolation of monoclonal antibodies specific for human c-*myc* proto-oncogene product. Mol. Cell. Biol. **5:**3610–3616.
17. **Evan, G. I., A. H. Wyllie, C. S. Gilbert, T. D. Littlewood, H. Land, M. Brooks, C. M. Waters, L. Z. Penn, and D. C. Hancock.** 1992. Induction of apoptosis

in fibroblasts by c-myc protein. Cell **69:**119–128.
18. **Galaktionov, K., X. Chen, and D. Beach.** 1996. Cdc25 cell-cycle phosphatase as a target of c-myc. Nature **382:**511–517.
19. **Gaubatz, S., A. Meichle, and M. Eilers.** 1994. An E-box element localized in the first intron mediates regulation of the prothymosin alpha gene by c-myc. Mol. Cell. Biol. **14:**3853–3862.
20. **Grandori, C., J. Mac, F. Siebelt, D. E. Ayer, and R. N. Eisenman.** 1996. Myc-Max heterodimers activate a DEAD box gene and interact with multiple E box-related sites *in vivo*. EMBO J. **15:**4344–4357.
21. **Griep, A. E., and H. F. DeLuca.** 1986. Decreased c-myc expression is an early event in retinoic acid-induced differentiation of F9 teratocarcinoma cells. Proc. Natl. Acad. Sci. USA **83:**5539–5543.
22. **Grosse, F., H. P. Nasheuer, S. Scholtissek, and U. Schomburg.** 1986. Lactate dehydrogenase and glyceraldehyde-phosphate dehydrogenase are single-stranded DNA-binding proteins that affect the DNA-polymerase-alpha-primase complex. Eur. J. Biochem. **160:**459–467.
23. **Guadagno, T. M., and R. K. Assoian.** 1991. G1/S control of anchorage-independent growth in the fibroblast cell cycle. J. Cell Biol. **115:**1419–1425.
24. **Han, E. K., T. M. Guadagno, S. L. Dalton, and R. K. Assoian.** 1993. A cell cycle and mutational analysis of anchorage-independent growth: cell adhesion and TGF-beta 1 control G1/S transit specifically. J. Cell Biol. **122:**461–471.
25. **Hanson, K. D., M. Shichiri, M. R. Follansbee, and J. M. Sedivy.** 1994. Effects of c-myc expression on cell cycle progression. Mol. Cell. Biol. **14:**5748–5755.
26. **Hoang, A. T., K. J. Cohen, J. F. Barrett, D. A. Bergstrom, and C. V. Dang.** 1994. Participation of cyclin A in Myc-induced apoptosis. Proc. Natl. Acad. Sci. USA **91:**6875–6879.
27. **Hoang, A. T., B. Lutterbach, B. C. Lewis, T. Yano, T. Y. Chou, J. F. Barrett, M. Raffeld, S. R. Hann, and C. V. Dang.** 1995. A link between increased transforming activity of lymphoma-derived MYC mutant alleles, their defective regulation by p107, and altered phosphorylation of the c-Myc transactivation domain. Mol. Cell. Biol. **15:**4031–4042.
28. **Hubank, M., and D. G. Schatz.** 1994. Identifying differences in mRNA expression by representational difference analysis of cDNA. Nucleic Acids Res. **22:**5640–5648.
29. **Jansen-Durr, P., A. Meichle, P. Steiner, M. Pagano, K. Finke, J. Botz, J. Wessbecher, G. Draetta, and M. Eilers.** 1993. Differential modulation of cyclin gene expression by MYC. Proc. Natl. Acad. Sci. USA **90:**3685–3689.
30. **Jones, R. M., J. Branda, K. A. Johnston, M. Polymenis, M. Gadd, A. Rustgi, L. Callanan, and E. V. Schmidt.** 1996. An essential E box in the promoter of the gene encoding the mRNA cap-binding protein (eukaryotic initiation factor 4E) is a target for activation by c-myc. Mol. Cell. Biol. **16:**4754–764.
31. **Kato, G. J., and C. V. Dang.** 1992. Function of the c-Myc oncoprotein. FASEB J. **6:**3065–3072.
32. **Leder, P., J. Battey, G. Lenoir, C. Moulding, W. Murphy, H. Potter, T. Stewart, and R. Taub.** 1983. Translocations among antibody genes in human cancer. Science **222:**765–771.
33. **Lee, L. A., C. Dolde, J. Barrett, C. S. Wu, and C. V. Dang.** 1996. A link between c-Myc-mediated transcriptional repression and neoplastic transformation. J. Clin. Invest. **97:**1687–1695.
34. **Lewis, B. C., and C. V. Dang.** Unpublished data.
35. **Li, L. H., C. Nerlov, G. Prendergast, D. MacGregor, and E. B. Ziff.** 1994. c-Myc represses transcription in vivo by a novel mechanism dependent on the initiator element and Myc box II. EMBO J. **13:**4070–4079.
36. **Liang, P., and A. B. Pardee.** 1992. Differential display of eukaryotic messenger RNA by means of the polymerase chain reaction. Science **257:**967–971.
37. **Lisitsyn, N., N. Lisitsyn, and M. Wigler.** 1993. Cloning the differences between two complex genomes. Science **259:**946–951.
38. **Lombardi, L., E. W. Newcomb, and R. Dalla-Favera.** 1987. Pathogenesis of Burkitt's lymphoma: expression of an activated c-myc oncogene causes the tumorigenic conversion of EBV-infected human B lymphoblasts. Cell **49:**161–170.
39. **Mai, S., and A. Jalava.** 1994. c-Myc binds to 5′ flanking sequence motifs of the dihydrofolate reductase gene in cellular extracts: role in proliferation. Nucleic Acids Res. **22:**2264–273.
40. **Miltenberger, R. J., K. A. Sukow, and P. J. Farnham.** 1995. An E-box-mediated increase in cad transcription at the G_1/S-phase boundary is suppressed by inhibitory c-Myc mutants. Mol. Cell. Biol. **15:**2527–2535.
41. **Nowell, P. C., and C. M. Croce.** 1986. Chromosomal approaches to the molecular basis of neoplasia. Symp. Fundam. Cancer Res. **39:**17–29.
42. **Packham, G., and J. L. Cleveland.** 1995. c-Myc and apoptosis. Biochim. Biophys. Acta **1242:**11–28.
43. **Pena, A., C. D. Reddy, S. Wu, N. J. Hickok, E. P. Reddy, G. Yumet, D. R. Soprano, and K. J. Soprano.** 1993. Regulation of human ornithine decarboxylase expression by the c-Myc.Max protein complex. J. Biol. Chem. **268:**27277–27285.
44. **Philipp, A., A. Schneider, I. Vasrik, K. Finke, Y. Xiong, D. Beach, K. Alitalo, and M. Eilers.** 1994. Repression of cyclin D1: a novel function of MYC. Mol. Cell. Biol. **14:**4032–4043.
45. **Prendergast, G. C., and E. B. Ziff.** 1992. A new bind for Myc. Trends Genet. **8:**91–96.
46. **Roberts, B. T., K. A. Farr, and M. A. Hoyt.** 1994. The *Saccharomyces cerevisiae* checkpoint gene *BUB1* encodes a novel protein kinase. Mol. Cell. Biol. **14:**8282–8291.
47. **Roy, A. L., C. Carruthers, T. Gutjahr, and R. G. Roeder.** 1993. Direct role for Myc in transcription initiation mediated by interactions with TFII-I. Nature **365:**359–361.
48. **Roy, A. L., M. Meisterernst, P. Pognonec, and R. G. Roeder.** 1991. Cooperative interaction of an initiator-binding transcription initiation factor and the helix-loop-helix activator USF. Nature **354:**245–248.
49. **Sambrook, J., E. F. Fritsch, and T. Maniatis.** 1989. Molecular cloning: a laboratory manual, 2nd ed. Cold Spring Harbor Laboratory, Cold Spring Harbor, N.Y.
50. **Schutte, B., M. M. Reynders, C. L. van Assche, P. S. Hupperets, F. T. Bosman, and G. H. Blijham.** 1987. An improved method for the immunocytochemical detection of bromodeoxyuridine labeled nuclei using flow cytometry. Cytometry **8:**372–376.
51. **Semsei, I., S. Y. Ma, and R. G. Cutler.** 1989. Tissue and age specific expression of the myc proto-oncogene family throughout the life span of the C57BL/6J mouse strain. Oncogene **4:**465–471.
52. **Seth, A., S. Gupta, and R. J. Davis.** 1993. Cell cycle regulation of the c-Myc transcriptional activation domain. Mol. Cell. Biol. **13:**4125–4136.
53. **Sharief, F. S., S. H. Wilson, and S. S. Li.** 1986. Identification of the mouse low-salt-eluting single-stranded DNA-binding protein as a mammalian lactate dehydrogenase-A isoenzyme. Biochem. J. **233:**913–916.
54. **Shim, H., C. E. Dolde, B. C. Lewis, C.-S. Wu, G. Dang, R. A. Jungmann, R. Dalla-Favera, and C. V. Dang.** 1997. c-Myc trans-activation of *LDH-A*: implications for tumor metabolism and growth. Proc. Natl. Acad. Sci. USA **94:**6658–6663.
55. **Smale, S. T., and D. Baltimore.** 1989. The "initiator" as a transcription control element. Cell **57:**103–113.
56. **Stone, J., T. de Lange, G. Ramsay, E. Jakobovits, J. M. Bishop, H. Varmus, and W. Lee.** 1987. Definition of regions in human c-myc that are involved in transformation and nuclear localization. Mol. Cell. Biol. **7:**1697–1709.
57. **Strickland, S., and V. Mahdavi.** 1978. The induction of differentiation in teratocarcinoma stem cells by retinoic acid. Cell **15:**393–403.
58. **Tavtigian, S. V., S. D. Zabludoff, and B. J. Wold.** 1994. Cloning of mid-G1 serum response genes and identification of a subset regulated by conditional myc expression. Mol. Biol. Cell **5:**375–388.
59. **Wagner, A. J., C. Meyers, L. A. Laimins, and N. Hay.** 1993. c-Myc induces the expression and activity of ornithine decarboxylase. Cell Growth Differ. **4:**879–883.
60. **Yang, B. S., T. J. Geddes, R. J. Pogulis, B. de Crombrugghe, and S. O. Freytag.** 1991. Transcriptional suppression of cellular gene expression by c-Myc. Mol. Cell. Biol. **11:**2291–2295.
61. **Zimmerman, K. A., G. D. Yancopoulos, R. G. Collum, R. K. Smith, N. E. Kohl, K. A. Denis, M. M. Nau, O. N. Witte, D. Toran-Allerand, C. E. Gee, et al.** 1986. Differential expression of myc family genes during murine development. Nature **319:**780–783.